

A simple design method for concrete fuse blocks at small dam spillways

Kawthar Achary¹, Sébastien Mawet², Pierre Archambeau³, Benjamin Dewals⁴, Michel Piroton⁵, and Sébastien Erpicum⁶

Abstract

Concrete fuse blocks are a promising cost-effective solution for enhancing small dam safety while increasing their storage capacity. This is especially needed in regions facing critical challenges due to limited water resources and the less rigorous design standards typically applied to small dams. Developed by the NGO HydroCoop, this technology is designed for installation on free-flow spillways. To enable large-scale implementation, a practical and safe design method is required—a method that is currently lacking. To address this gap, an analytical model was developed to predict the fuse block tipping head based on the physical stability of the block, and was validated with experimental data. Systematic tests were conducted at laboratory scale (1/10 scale factor) using six blocks with varying widths (dimension perpendicular to the flow direction). These blocks were tested in two configurations—alone on the weir or with adjacent blocks—and in two positions: at the center or on the side of the weir. The tests enabled the determination of the blocks' tipping head. A standard block geometry was defined and used alongside the model to create a simple design table. This table allows practitioners to determine the appropriate fuse block height based on two input parameters—block density and head over the spillway crest—without requiring complex calculations. A dedicated discussion addresses the practical implications and limitations of fuse blocks, including the intensity of discharges generated when the blocks tip, the risk of earlier-than-expected tipping, and the usable storage range. Additional experimental validation is nonetheless needed to refine the method for non-standard geometries. A future research perspective is also to investigate the potential structural consequences of block tipping, both on the spillway and downstream.

Keywords

Hydraulic modeling, scale model, design equation, reservoir, dam development

¹kawthar.achary@uliege.be; University of Liège, Liège, Belgium

²smawet@uliege.be; University of Liège, Liège, Belgium

³pierre.archambeau@uliege.be; University of Liège, Liège, Belgium

⁴b.dewals@uliege.be; University of Liège, Liège, Belgium


⁵michel.piroton@uliege.be; University of Liège, Liège, Belgium

⁶s.erpicum@uliege.be; University of Liège, Liège, Belgium

Research Article. **Submitted:** 27 January 2025. **Reviewed:** 1 April 2025. **Accepted** after double-anonymous review: 26 May 2025. **Published:** 09 July 2025.

DOI: <https://doi.org/10.59490/jchs.2025.0045>

Cite as: Achary, K., Mawet, S., Archambeau, P., Dewals, B., Piroton, M., Erpicum, S., A simple design method for concrete fuse blocks at small dam spillways, Journal of Coastal and Hydraulic Structures, 45, DOI: <https://doi.org/10.59490/jchs.2025.0045>

The Journal of Coastal and Hydraulic Structures is a community-based, free, and open access journal for the dissemination of high-quality knowledge on the engineering science of coastal and hydraulic structures. This paper has been written and reviewed with care. However, the authors and the journal do not accept any liability which might arise from use of its contents. Copyright © 2025 by the authors. This journal paper is published under a CC BY 4.0 license, which allows anyone to redistribute, mix and adapt, as long as credit is given to the authors. 

ISSN: 2667-047X online

1 Introduction

1.1 Background

Water is essential to life. All vital activities such as agriculture, livestock farming, human water supply and construction are particularly dependent on surface water (Durand et al., 1999; Kabore et al., 2015; World Bank, 2021). However, its availability varies considerably over time and space. Given this variability, reservoirs play a crucial role in storing water for later use. Large dams provide a safe and reliable solution for water storage and management. The World Register of Dams (ICOLD, 2023) lists 61,988 large dams. However, their high construction costs often drive dam managers to favour the implementation of small dams (World Bank, 2021). Although there is no universal definition for small dams, they are generally considered to be all dams that do not meet the criteria for large dams. A large dam is defined by the International Commission on Large Dams (ICOLD) as one that is more than 15 meters in height from the lowest foundation to the crest, or between 5 and 15 meters in height while retaining more than 3 million cubic meters of water (ICOLD, 2011). Information on the number of small dams is sometimes undocumented, complicating global estimates (Güven and Aydemir, 2020). In each country, the number of small dams exceeds that of large dams (Güven and Aydemir, 2020), and according to World Bank (2021), it may reach millions globally. These smaller dams follow less rigorous design and construction standards and have lower operation and maintenance requirements compared to large dams (Güven and Aydemir, 2020; World Bank, 2021; Pinto and Ferreira Fais, 2023). Small dams receive significantly less attention than large ones, as their construction tends to focus on economic considerations and cost savings (ICOLD, 2016). Small dam failures are more frequently reported than those of large dams, partly due to their overwhelming number. In the United States, over 93% of dams are less than 15 meters high (National Performance of Dams Program, 2018). According to the National Performance of Dams Program (NPDP) database, between 1848 and 2017, there were 1,645 recorded dam failures, of which 1,546 involved dams under 15 meters in height (National Performance of Dams Program, 2018). This means that 94% of dam failures concerned small dams, which is roughly proportional to their number. Therefore, while small dams fail more often in absolute numbers, their relative failure rate might not be significantly higher than that of large dams. Nevertheless, the failure of small dams can still lead to severe accidents and significant damage to local populations (Pinto and Ferreira Fais, 2023).

Spillways play a central role in dam safety by enabling controlled release of excess water from the reservoir. Their primary function is to prevent the water level from exceeding safe limits, which could otherwise lead to downstream flooding or structural damage (Salunkhe et al., 2020). A well-sized spillway provides continuous flood protection and prevents hydraulic overload, enhancing the resilience of the dam during extreme events.

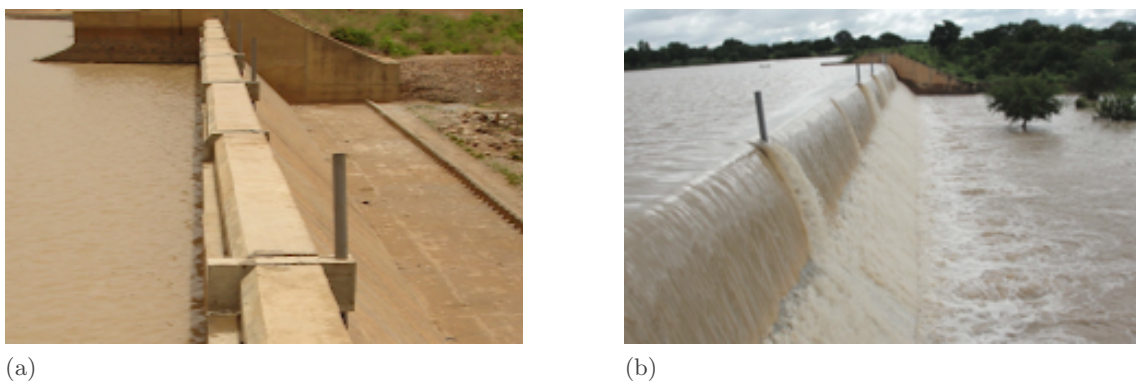


Figure 1: Concrete fuse blocks installed on the Wedbila small dam spillway in Burkina Faso: (a) before submersion (adapted from Lempérière (2017)), and (b) during submersion (from Hydrocoop (2015)).

The fuse blocks (Fig. 1) developed by HydroCoop (Hydrocoop, n.d.) improve the design of free-flow spillways for small dams. Placed side by side on the spillway crest, these concrete blocks tilt and fall downstream when the water level reaches a specific point, thereby disappearing from the spillway crest (Lempérière and Vigny, 2013). This tipping mechanism is passive and relies solely on the hydraulic head: as long as the reservoir water level remains below the tipping threshold, the blocks remain submerged and stable (Figure 1b). Once the water level reaches the critical tipping point, the hydraulic force exerted on the block induces its rotation. Since the blocks are neither fixed nor attached to the spillway crest, they pivot around a defined point at their downstream edge and fall freely downstream. This mechanism enables a sudden and automatic increase in spillway discharge capacity, without any mechanical system or human intervention.

This system increases water storage capacity by raising the spillway crest without impacting the dam safety. This is useful for restoring lost storage capacity due to sedimentation for instance. Thus, these blocks give a second life to dams that might otherwise be less effective or obsolete. Moreover, as the fuse blocks increase the storage capacity, they also help to meet growing water demand while maintaining safety by restoring the initial discharge capacity when the blocks fall from the spillway crest. They can also be used to lower an existing spillway crest while maintaining storage capacity and thus improving flood discharge capacity. The technology is therefore a cost-effective alternative to gated spillways, offering flexibility in handling various flood scenarios (Lempérière, 2017). A detailed geometry of fuse blocks is provided in Figure 2.

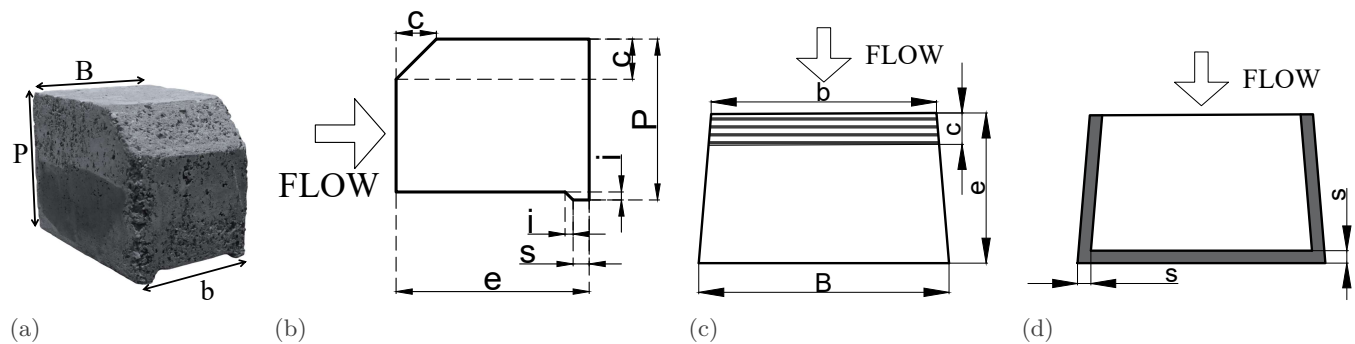


Figure 2: Block geometry: (a) Picture of a fuse block. (b) Cross-section. (c) Plan view of upper face. (d) Plan view of lower face. P is the block height; B is the downstream (D/S) width (perpendicular to flow direction); b is the upstream (U/S) width (perpendicular to flow direction); e is the block length (in flow direction); i is the height of the block underpressure chamber; c is the block chamfer height and length; s is the width of block supports delimiting the underpressure chamber.

Operation of a fuse block results from an equilibrium between its weight (stabilisation force) and water pressure (mainly destabilisation force). To accurately predict the water level at which tipping occurs, it is essential to precisely determine the pressure beneath the block. This can be achieved either by completely preventing underpressure (with a watertight seal upstream and an opening downstream, resulting in atmospheric pressure) or by allowing full pressure development (with a watertight seal downstream and an opening upstream, allowing reservoir pressure) (Lempérière and Vigny, 2013).

Two designs of blocks are proposed by Hydrocoop: blocks that tilt before their submergence and blocks that tilt after. The first are designed by making them relatively tall compared to their width, with a no-underpressure solution to reduce length e . The second, that tilt after being submerged by a water height “ $H_{Tipping}$ ” (up to 2 times their height P), are relatively wide and long (B/P up to 10; e/P up to 3). In this configuration, a total underpressure solution is preferred to offer better tilting accuracy, although it consumes more concrete (Lempérière and Vigny, 2013). The present work focused on blocks with a total underpressure solution.

It is recommended by precedent studies (Lempérière and Vigny, 2013) to chamfer the upstream face (illustrated in Figure 2 by the length and width c) of the blocks to improve discharge capacity and decrease discharge variation during tilting. To prevent that the tilting of one block affects adjacent blocks, a thin wall between adjacent blocks is beneficial. Experimental tests carried out in various countries (France, Algeria, China, Vietnam, and coordinated by HydroCoop) indicate that these separators are effective, particularly for narrow blocks, and their lengths are typically chosen to be equal to 1.2 times the length e of the block. To minimise friction caused by manufacturing defects, it is recommended to slightly reduce the width b of the upstream face, creating a trapezoidal shape (Lempérière and Vigny, 2013). Blocks should be positioned upstream of a small abutment to prevent them from sliding. This abutment also serves as a pivot point around which the block rotates when subjected to hydrodynamic forces. In practice, all blocks on the same weir usually have the same height but may vary in length, which allows them to tilt at different water levels in the reservoir (ICOLD, 2010).

Fuse blocks are currently used in countries like Burkina Faso and Vietnam. An example is the Gaskaye dam in Burkina Faso (Kabore et al., 2015), a small earth-fill dam 464 m long and with a useful maximal height of 2.9 m. It has a reservoir capacity of 1,353,000 m³ and features a free overflow spillway measuring 100.15 m. However, this reservoir’s capacity has become inadequate for local needs due to population growth and a gradual loss of storage caused by sedimentation. To address this, five groups of three concrete fuse plugs, each 0.30 m high, were installed, with lengths e ranging from 0.55 m to 0.9 m and a width of 6.30 m. These blocks have an upstream width b equal to the downstream width B . Another example is the Wedbila dam in Burkina Faso (Hydrocoop, 2013). This small

earth-fill dam is 600 m long and has a useful maximal height of 4 m, with a storage capacity of 2 million m³. The dam is primarily used for irrigation and also supplies water for livestock, domestic use, and construction needs of nearby communities during the dry season. Similar to Gaskaye, Wedbila faces storage capacity challenges. Its spillway, 70 m in width, was raised by adding concrete fuse plugs, each 0.50 m high, with lengths e between 0.78 m and 1.03 m, and a width of around 9.6 m. The upstream width b equals the downstream width B . In both projects, the increased normal water level boost reservoir storage capacity by 25%. For each dam, the first fuse blocks are designed to tilt under a 10-year flood event. The water head above the block that induces tilting $H_{Tipping}$ is provided in Table 1 for both dams.

Table 1: Tipping water head $H_{Tipping}$ values for the Gaskaye (Kabore et al., 2015) and Wedbila (Hydrocoop, 2013) dams regarding the block length.

Gaskaye dam						Wedbila dam							
Length e [cm]	55	60	67.5	75	90	Length e [cm]	78	82	85	89	94	98	103
$H_{Tipping}$ [cm]	50	54.6	60.3	64.8	71.2	$H_{Tipping}$ [cm]	66	70	74	78	82	86	90

1.2 Existing design methods

To design those blocks, two equations can be found in the literature (Hien and Ho Ta Khanh, 2007; Sekkour, 2016). They are both analytically derived from the static equilibrium of a fuse block around the rotation point O . They differ by the assumptions made on the pressure distributions acting on the block faces and by the simplification of the block geometry.

Hien and Ho Ta Khanh (2007) studied underpressure fuse blocks, focusing on accurately determining the water level needed to tip them. They used blocks with a geometry similar to that studied by Lempérière and Vigny (2013) and tested them in a 34 m long, 0.6 m wide, and 0.65 m high glass flume. Two configurations were tested. The first used three fuse blocks of equal width ($B = 18.8$ cm) across the entire weir, with lengths e varying from 10 to 20 cm and separated by walls, and the second used two blocks of equal width ($B = 29$ cm) across the weir, with the same length variations and wall separations. Thanks to a piezometer, they measured the depth H_{block} 1.2 m upstream of the blocks. They proposed a simple calculation method based on pressure distribution assumptions, shown in Figure 3a. The resultant pressures (Figure 3b) were determined by integrating the pressure distributions over the corresponding surfaces and their point of application was calculated by taking the weighted averages of the pressures. An equilibrium of the moments induced by the forces in Figure 3b led to the following formula:

$$H_{Tipping} = \frac{-6Me + \rho_w(P - i) \cdot [2B(P - i) \cdot (P + 2i) + 3(B + b)e^2]}{3\rho_w \cdot [-2B \cdot (P^2 - i^2) + (\beta - 1)(B + b)e^2]} \quad (1)$$

where $H_{Tipping}$ is the minimum calculated height necessary to causes the block to tip, M corresponds to the mass of the fuse block, ρ_w is the density of water and β is a reduction factor [-] used to account for the water height on the block being a percentage of the upstream head H_{block} . Note that $H_{Tipping}$ represents the height 1.2 m upstream of the block and that its reference level is the block height, therefore corresponding to a water depth above the block, but 1.2 m upstream.

Hien and Ho Ta Khanh (2007) concluded that, for a given block cross-section, the block width does not affect the tipping height. For thin sills ($e/P < 1$), β takes a value of around 0.2, and for wide sills ($e/P > 1$), β ranges from 0.6 to 0.65. These values are specific to the block geometry they studied. They suggest that the block height of real prototypes should generally not exceed 1 m to limit the block length e and therefore block weight. This approach, while considering the previously described geometry in their experiments, does not account for the presence of chamfers, leading to discontinuities in the pressure distribution from one face to another and pressures not orthogonal to the chamfer surface.

In his master's thesis, Sekkour (2016) also developed a formula (Eq. 2) to design fuse blocks based on their geometric parameters, using a momentum equilibrium of forces derived from specific pressure distribution assumptions (see Figure 4a for a representation of the pressure distribution assumptions and Figure 4b for the resulting forces). The blocks studied in this work do not correspond to the previous description suggested by Lempérière and Vigny (2013). These are very simple blocks that are not chamfered upstream and do not have a reduced upstream width compared to the downstream width. Nine fuse blocks of the same height ($P = 10$ cm) and width ($B = 20$ cm) with lengths e varying from 8.2 cm to 14.9 cm were considered. To validate the design equation, model blocks were tested in a 4 m wide, 5 m long, and 1.5 m deep reservoir. Two configurations were tested: first, a weir allowing the placement of a single block, and second, a weir allowing the placement of three blocks separated by intermediate walls as high as those

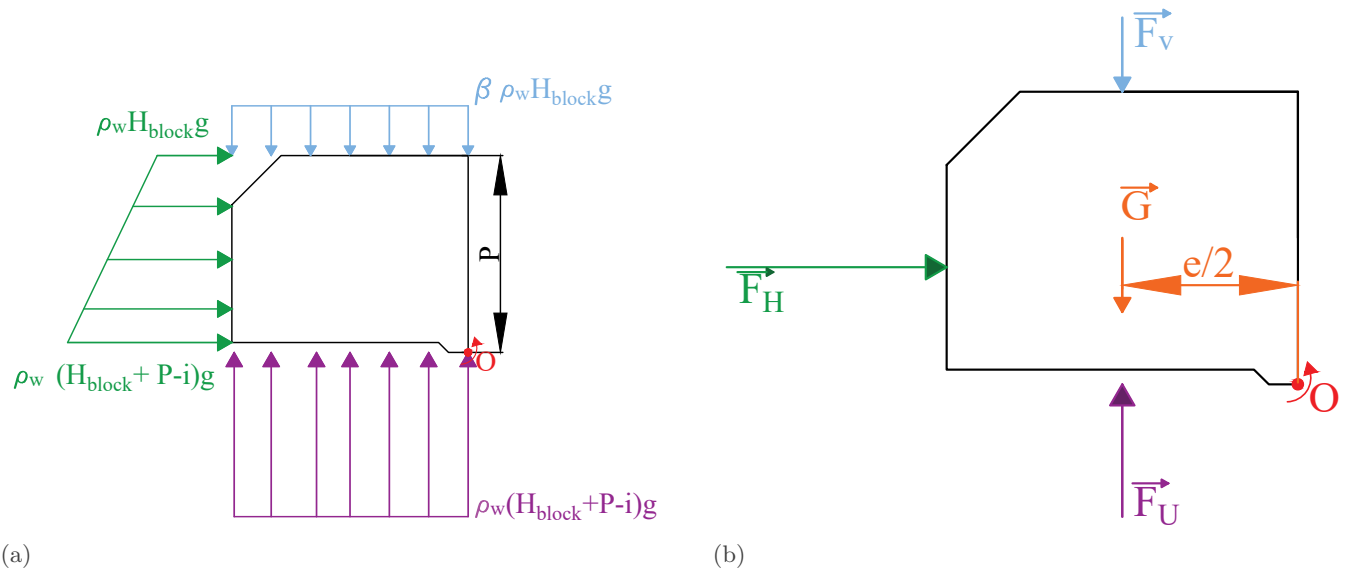


Figure 3: Hien and Ho Ta Khanh (2007) model: (a) Hydrostatic pressure distribution assumptions. (b) Force diagram. The pressures shown in (a) are integrated over the corresponding surfaces. The resultant forces are: \vec{F}_U from underpressure on the bottom face, \vec{F}_H from horizontal pressure on the upstream face, and \vec{F}_V from vertical pressure on the top face. The weight \vec{G} , is applied at a horizontal distance $e/2$ from the rotation point O .

on each side of the weir. The experimental data closely matched the theoretical predictions, showing that the tipping height increased with block length e . This was confirmed by the configuration testing the tipping of three blocks of different lengths e simultaneously. Indeed, the blocks tipped one at a time at their respective tipping heights: first the block with the smallest e and last the block with the largest e . The results obtained in the first configuration, with the tipping of a single block, were relatively similar to those in the second configuration, regardless of the block's position on the weir (middle or side). This analytical model, despite its simple block geometry, does not ensure continuous pressure at the upper upstream corner of the block.

$$H_{\text{Tipping}} = \frac{3Pe^2 \left(\frac{\gamma_b - \gamma_w}{\gamma_w} \right) - P^3}{e^2 + 3P^2} \quad (2)$$

where γ_w and γ_b are the specific weights of water and the concrete fuse block, respectively.

Despite these two promising studies, some questions remain unsettled. On one hand, Hien and Ho Ta Khanh (2007) studied a block geometry similar to the one proposed by Lempérière and Vigny (2013), specifically with a chamfer. However, their experiments took place in a flume, which does not fully reflect the conditions in a reservoir. Indeed, in a flume, the water level varies more rapidly to discharge fluctuations, *i.e.* to weir geometry variations during tilting, than in a reservoir. Moreover, their analytical model does not take the chamfer into account. On the other hand, Sekkour (2016) developed a simpler formula considering a rectangular parallelepiped geometry but verified it using tests that more closely represent a dam reservoir. This raises the question of whether these models are representative in more general situations, especially when the block geometry is more complex and in reservoir conditions.

In this work, experiments were conducted to determine the tipping behaviour of fuse blocks respecting Lempérière and Vigny (2013) geometry placed in a reservoir configuration. Based on these results, an analytical model using force equilibrium is proposed to efficiently size the fuse blocks. This model considers the chamfer and therefore the exact geometry of the block and uses continuous pressure diagrams between the faces, providing a simple equation that relates block geometry to tilting parameters.

The paper is organised as follows. First, in Section 2, the experimental setup and test protocol are described. The analytical model and the underlying assumptions are presented in Section 3. Then, Section 4 provides the experimental results, which are compared with predictions from existing models and the newly developed one. Next, in Section 5, the results, along with the practical implications and limitations of fuse blocks, are discussed. In Section 6, a new design method is proposed—detailed, simple, and safe with regard to dam overtopping. Finally, a general conclusion is drawn in Section 7.

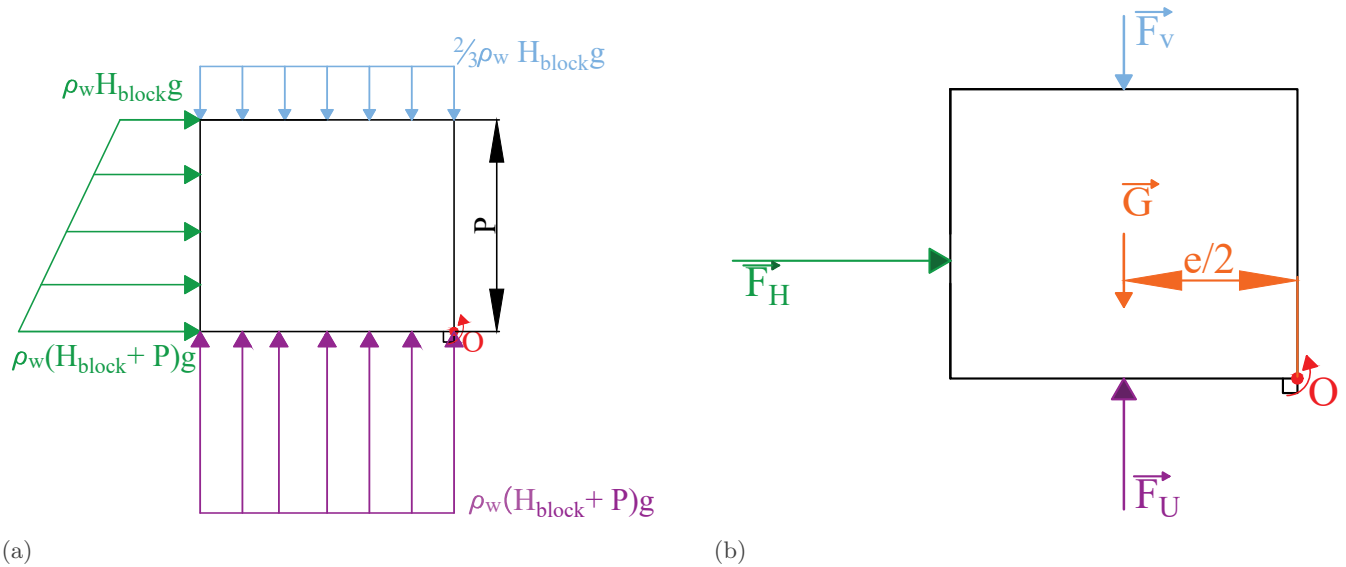


Figure 4: Sekkour (2016) model: (a) Hydrostatic pressure distribution assumptions. (b) Force diagram. The pressures shown in (a) are integrated over the corresponding surfaces. The resultant forces are: \vec{F}_U from underpressure on the bottom face, \vec{F}_H from horizontal pressure on the upstream face, and \vec{F}_v from vertical pressure on the top face. The weight \vec{G} , is applied at a horizontal distance $e/2$ from the rotation point O .

2 Methodology

2.1 Experimental setup

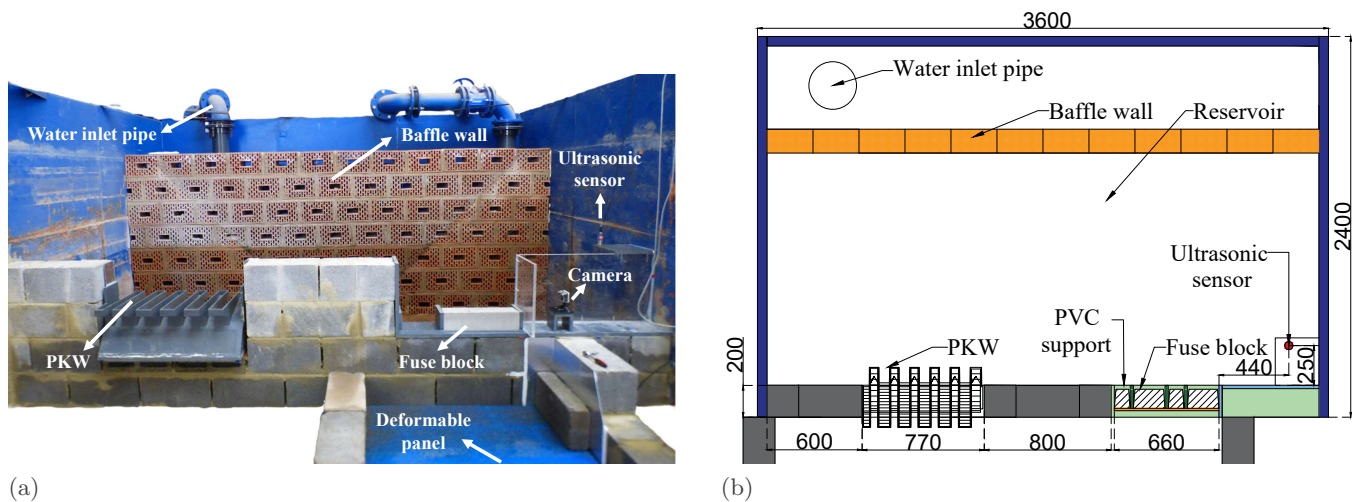


Figure 5: Views of the experimental setup: (a) Picture of the system components. (b) Plan view of the model with the dimensions [mm].

The experimental setup aims to represent a reservoir with a wide surface, *i.e.* a level which does not vary abruptly with discharge variations. To reproduce this, two spillways have been built side by side: fuse blocks placed on a broad crested weir and a piano key weir (Fig. 5).

Water discharge is supplied to the experimental setup through an inlet pipe of 0.15m diameter. A baffle wall helps uniformize the water's kinetic energy before the flow enters the reservoir. The 2.4 to 3.6 m reservoir is made of metal walls on three of its sides and a masonry wall on the fourth one. A part of the masonry wall is replaced by a plexiglass panel to observe the water level in the reservoir and the cross-section of the blocks. It also serves as a support for a camera. A large discharge capacity weir (Piano Key Weir (PKW)) maintains an almost constant water level despite

variations in discharge over the fuse blocks. The hydraulic head on the fuse blocks is calculated from the reservoir level, neglecting flow velocity. This is justified by the large cross-section of the reservoir relative to the discharge.

To analyse the behaviour of fuse blocks, the time evolution of two key parameters is collected: the hydraulic head and the discharge. The upstream head H_{block} acting on a block is measured with an ultrasonic sensor (Microsonic VNP-35/IU/TC with millimetre accuracy) placed 25 cm upstream and 44 cm on the left of the weir. This location avoids the contraction and acceleration zone near the upstream face of the weir and ensures that the local flow velocity remains negligible, given both the measurement location in a reservoir corner and the limited discharge relative to the reservoir dimensions. The probe is connected to a data acquisition box that transmits information to a computer, where LabVIEW software records data at 10 Hz. The flow rate injected into the reservoir is measured with a flowmeter (SITRANS FM MAG 5000 with accuracy of 0.5% FS) installed on the water pipe, also connected to LabVIEW. Voltage signals from the ultrasonic sensor and flowmeter are converted to water level and flow rate using a MATLAB routine.

The blocks are designed with a geometric scale appropriate for laboratory use, while minimizing scale effects, *i.e.* with a height of 0.1 m, corresponding to a geometric ratio between the model blocks and the real ones ranging from 1:5 to 1:10. The blocks were initially placed on a 0.66 m wide broad-crested weir located on the left-hand side of the masonry wall, allowing placement options at the side or centre. To expand testing, the weir was later widened to 1.224 m. Blocks can be fixed using plasticine, a malleable and removable material. The study involved six blocks subjected to underpressure, all having the same cross-section but varying in width from 10 to 60 cm. The block geometry is illustrated in Figure 2 and dimensions are provided in Table 2. The mass of the blocks was measured accurately, while the ranges in density resulted from uncertainty in the lengths (measurement accuracy of 1 mm).

Table 2: Geometric and physical parameters of the six types of blocks studied (B10 to B60). The density ranges reflect the uncertainty of the length measurements.

	B10	B20	B30	B40	B50	B60
Height P [cm]	10 ± 0.1	9.9 ± 0.1	9.8 ± 0.1	10 ± 0.1	9.8 ± 0.1	9.9 ± 0.1
U/S width b [cm]	7.9 ± 0.1	18.3 ± 0.1	28.3 ± 0.1	38.3 ± 0.1	48.2 ± 0.1	58.3 ± 0.1
D/S width B [cm]	10 ± 0.1	20 ± 0.1	30 ± 0.1	40 ± 0.1	50 ± 0.1	59.9 ± 0.1
Length e [cm]	12.1 ± 0.1	12 ± 0.1	12.1 ± 0.1	11.9 ± 0.1	12 ± 0.1	12 ± 0.1
Mass [kg]	2.315	4.923	7.2	10	12.5	14.9
Density range [kg/m ³]	2228-2377	2263-2333	2232-2278	2313-2348	2292-2319	2295-2318

All fuse blocks are chamfered on the upstream face with a 1:1 slope and a width c of 2.5 cm. In each concrete piece, a 0.5 cm-high opening, i , is made from the bottom corner, representing the underpressure chamber. On three sides of the element, 1cm-wide strip, identified as s , serves as support. Due to this configuration, the water enters the lower chamber through the upstream face.

The fuse blocks are placed on a PVC support, which allows for the attachment of abutments and intermediate walls. The abutment is a PVC element, 0.5 cm high and 1.5 cm wide, placed continuously along the weir width and screwed onto the PVC support. It prevents the blocks from sliding by physically blocking their movement in the flow direction. In addition, it defines the pivot point for block rotation under the action of the flow-induced forces. The separator walls have the same height as the blocks and are 14.4 cm long (1.2 times e). They are aligned with the upstream edge of the PVC support. To reduce contact between the blocks and adjacent walls, the upstream width of the blocks is 2 cm narrower than the downstream width. Folded plastic strips (see Fig. 6) are placed between the blocks and the intermediate walls to prevent water leaks and ensure that there is no lateral friction, thereby not affecting block tilting. To cushion the fall of the block and avoid damage, a deformable panel is placed downstream of the weir.

The discharge coefficient C_d of the blocks and the PKW has been determined by injecting various constant flow rates into the experimental setup and measuring the corresponding water level. This provided a direct analytical relation between the hydraulic head and the flow rate for each weir.

2.2 Test configurations and protocol

The experimental tests aim to determine the head required to topple a single block $H_{Tipping}$ in various configurations and positions. Two scenarios were tested. In the first configuration (Cfg. 1), the block is placed alone on the weir, leaving the rest of the sill empty. This setup replicates the condition when all adjacent elements have tipped over, and only one fuse block remains. This configuration is shown in Figure 7a and 7b. In the second configuration (Cfg. 2),

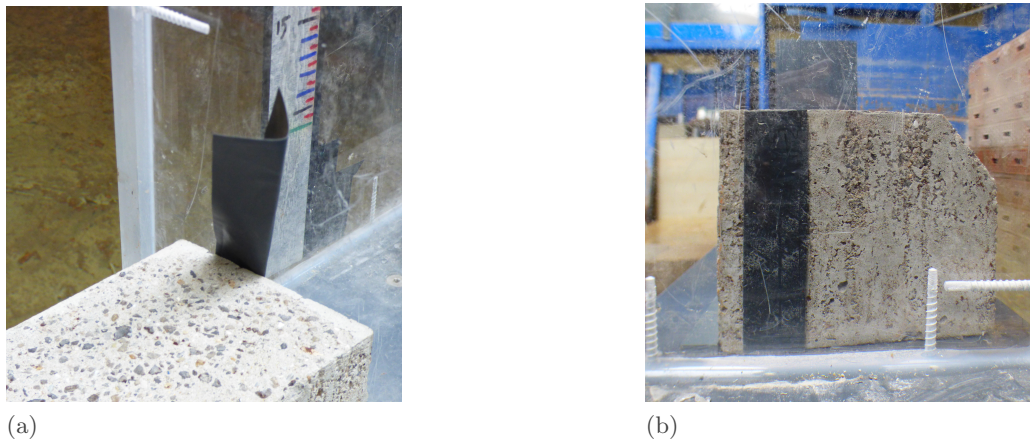


Figure 6: Pictures of the folded plastic strip between block and intermediate wall to prevent water leaks. (a) Picture of the installation of the folded plastic strip. (b) Picture of the folded plastic strip in place.

adjacent blocks are present and fixed. This setup corresponds to the scenario where the studied block is the first to topple. This is illustrated in Figure 7c and 7d.

For blocks B10 and B20, tests were conducted in two positions: first at the side of the weir (Figure 7a and 7c) and then in its centre (Figure 7b and 7d). For the other blocks, only one position was tested due to the weir limited size. The number of tests carried out, and the configurations studied for each block, are shown in Table 3.

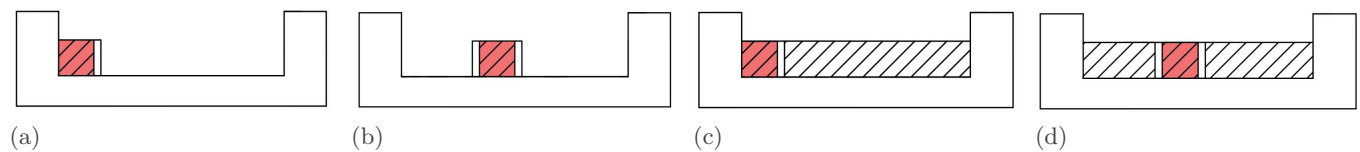


Figure 7: Diagrams of the test configurations: (a) Block alone on the weir (Cfg. 1) and positioned on the side. (b) Block alone and centered (Cfg. 1). (c) Block surrounded by fixed blocks on the weir (Cfg. 2) and positioned on the side. (d) Block surrounded by fixed blocks and centered (Cfg. 2). In all configurations, the tested block is represented in red, the fixed blocks are shown in white with hatching, and the intermediate walls are depicted in white.

Table 3: Summary of tests: Number of repetitions for each block type (B10 to B60, see Table 2 for their physical description) by configuration (Cfg. 1 or Cfg. 2) and block position (side or centre of the weir).

* Tests with the expanded weir (1.224 m wide)

Configuration	Placement	B10	B20	B30	B40	B50	B60
Cfg. 1	Side	6	3	18	5	4	5
	Centre	3	7*	-	-	-	-
Cfg. 2	Side	2	5	4	-	-	-
	Centre	3	5*	-	-	-	-

During a test, the studied fuse block is first placed between the intermediate walls. The watertight plastic strips are installed. Then, for configuration 2, adjacent blocks are fixed with plastiline. The experiment starts and the data acquisition begins simultaneously with the flow injection. The initial flow rate is chosen close to, but below, the one needed to destabilise the block. After this, the initial flow is increased in steps of 3-4 l/s every 60 s until the block topples. After the tilting, the data are recorded for an additional 30-60 s before ending the test.

2.3 Data processing

The experiments yield time evolution of flow rate and water height H_{block} . An example of a water height measurement, namely the initial signal, is shown in Figure 8. The obtained signals are noisy due to measurement method intrinsic limitations. An automatic procedure described below has been implemented to clean the data from outliers and smooth it. Additionally, since the flow rate is increased in steps, a method has been developed to determine values for each plateau in the water level, labelled as Plateaus in Figure 8. Note that a similar procedure has been applied to the discharge signal to obtain the discharge plateaus.

The procedure includes four steps:

- Replacement of outliers:** Outliers (values significantly different from the previous ones) are detected and replaced by linear interpolation between the two adjacent values to obtain the cleaned signal, yellow curve in Figure 8. They are identified by detecting variations equal or higher to 2 mm (equivalent to 3 l/s in flow rate) between adjacent values.
- Signal smoothing:** A moving average with a window size of 13 s is applied to reduce measurement noise and smooth the data (see the smoothed signal in Figure 8). The 13-second window was determined through trial and error to best match the general trend of the data.
- Identification of plateaus:** Detection of the plateaus (see plateaus in Figure 8) by comparing values within defined intervals. A measurement point is identified as belonging to a plateau if the difference between its instantaneous value and that of the previous measurement point does not exceed 0.02 mm (or 0.02 l/s for the flow rate).
- Calculation of average values:** Compute the average value for each identified plateau.

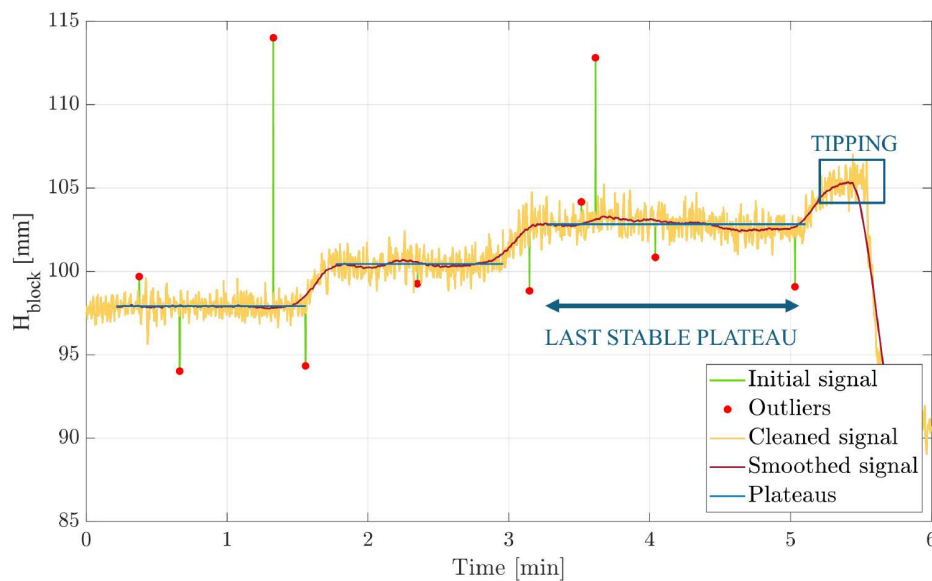


Figure 8: Data processing for hydraulic head signals: an initial signal (green) with outliers (red dots) is cleaned (yellow) and smoothed (purple curve). Plateaus (blue lines) are obtained by averaging data over time intervals to obtain a single value per level. The tipping moment of the fuse block is highlighted in blue and the last stable plateau identified.

Once each plateau, *i.e.* each stable reservoir level, has been defined by its average value, each reservoir level can be classified into one of three categories: Stable Head, Tipping Head, and Unstable Head:

- **Stable Head:** This is the last plateau before the block tilts, corresponding to the last stable stage in Figure 8. It represents the highest head at which the block remains stable.
- **Tipping Head:** If the block tilts while the head signal is constant, this head value causes the block to tip over.
- **Unstable Head:** If the block tips during an increasing flow phase (before reaching a plateau), the exact tipping head cannot be directly determined. Instead, the last recorded discharge level after tilting is used to compute

the associated head (using the head-discharge relationships), corresponding to the head at which the block has tilted.

3 Analytical model

To develop a simple design method, an analytical model based on the configuration described in Figure 2 and relating the geometric parameters of the block to its tipping is proposed. The model is based on balance of moments to determine the stability of the block. The forces responsible for these moments are of two kinds: those linked to the water pressures on the different faces of the block and the block's weight \vec{G} . The block tilts around an axis of rotation located at the downstream abutment at a distance i from its bottom (labelled O in Figure 10). The stability limit is determined when all moments counterbalance each other.

Calculations assume hydrostatic pressure distribution $\rho_w gh$, where ρ_w refers to the density of the fluid, g is the norm of the gravitational acceleration, and h is the water height. Water depth acting on the block upstream face is assumed to be directly related to the reservoir level (Figure 9). This simplification neglect kinetic energy in the reservoir (flow velocity is small due to limited discharge compared to reservoir dimensions) and neglect head loss between the reservoir and the weir.

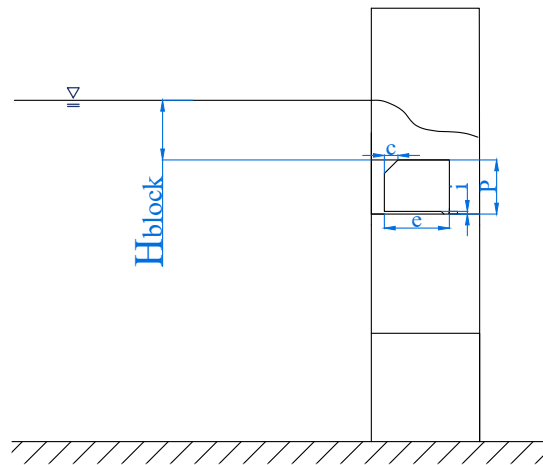


Figure 9: Diagram illustrating the upstream head of the block H_{block}

New assumptions about pressure distributions are introduced to ensure continuity along the block faces, as shown in Figure 10a:

- **Vertical pressure:** The flow exerts a uniform hydrostatic pressure on the block crest, equivalent to a percentage α of the upstream head. This coefficient α is initially assumed to be $\frac{2}{3}$. This assumption is justified as the block behaves like a broad-crested weir. In hydrostatic conditions, the critical depth is $\frac{2}{3}$ of the relative specific head of the flow. Hence, at first sight, choosing $\alpha = \frac{2}{3}$ seems reasonable, although it may not perfectly represent the case of profiled weirs, where pressure is no more hydrostatic.
- **Horizontal pressure:** A hydrostatic pressure directly proportional to the reservoir level is applied to the upstream face of the block. Considering the lower chamber, the head at the bottom corner is $H_{block} + P - i$.
- **Underpressure:** The underpressure is assumed to be uniform, applied on all the chamber surface.
- **Chamfer pressure:** The pressure diagram applied on the chamfer ensures pressure continuity on each face of the block.

The resultant forces due to pressure distributions are obtained by integrating the pressures over the surfaces, as illustrated in Figure 10b. The points of application of these forces are calculated as weighted averages of the pressure distributions. To determine the moments induced by these forces, the magnitudes of the forces are multiplied by their lever arms, which are the perpendicular distance between the block's rotation point O and the line of action of the force.

Finally, the **block weight** \vec{G} is applied at the centre of mass, which has been determined by taking the presence of the chamfer into account. The centre of mass is located at a horizontal distance X_{CG} from the point of rotation O (Eq. 3).

$$x_{CG} = \frac{e^2 \cdot (P - i) - c^2 \cdot (e - \frac{c}{3})}{2 \cdot e \cdot (P - i) - c^2} \quad (3)$$

Taking these assumptions into account, the equilibrium moment equation leads to the following relationship linking the theoretical tipping head $H_{Tipping}$ to the block properties:

$$H_{Tipping} = \frac{-(d_G + d_{c,stab} - d_H - d_U - d_{c,destab})}{C_v + C_{c,stab} - C_H - C_U - C_{c,destab}} \quad (4)$$

with

$$d_G = \rho_b \cdot g \cdot [(P - i) \cdot e - c^2/2] \cdot x_{CG}$$

$$d_{c,stab} = \frac{\gamma_w \cdot (3 \cdot c^2 \cdot e - c^3)}{6}$$

$$d_H = \frac{\gamma_w \cdot (P - c - i)^2 \cdot (P + 2c - i)}{6}$$

$$d_U = \frac{\gamma_w \cdot (P - i) \cdot (e^2 - s^2)}{2}$$

$$d_{c,destab} = \frac{\gamma_w \cdot c \cdot [3 \cdot (P - i - c) \cdot c + c^2]}{6}$$

$$C_v = \frac{\gamma_w \cdot (e - c)^2 \cdot \alpha}{2}$$

$$C_{c,stab} = \frac{\gamma_w \cdot c \cdot (5 \cdot e - 7/3 \cdot c)}{6}$$

$$C_H = \frac{\gamma_w \cdot (P - c - i)^2}{2}$$

$$C_U = \frac{\gamma_w \cdot (e^2 - s^2)}{2}$$

$$C_{c,destab} = \frac{\gamma_w \cdot c \cdot [(P - i - c) \cdot 5 + 7/3 \cdot c]}{6}$$

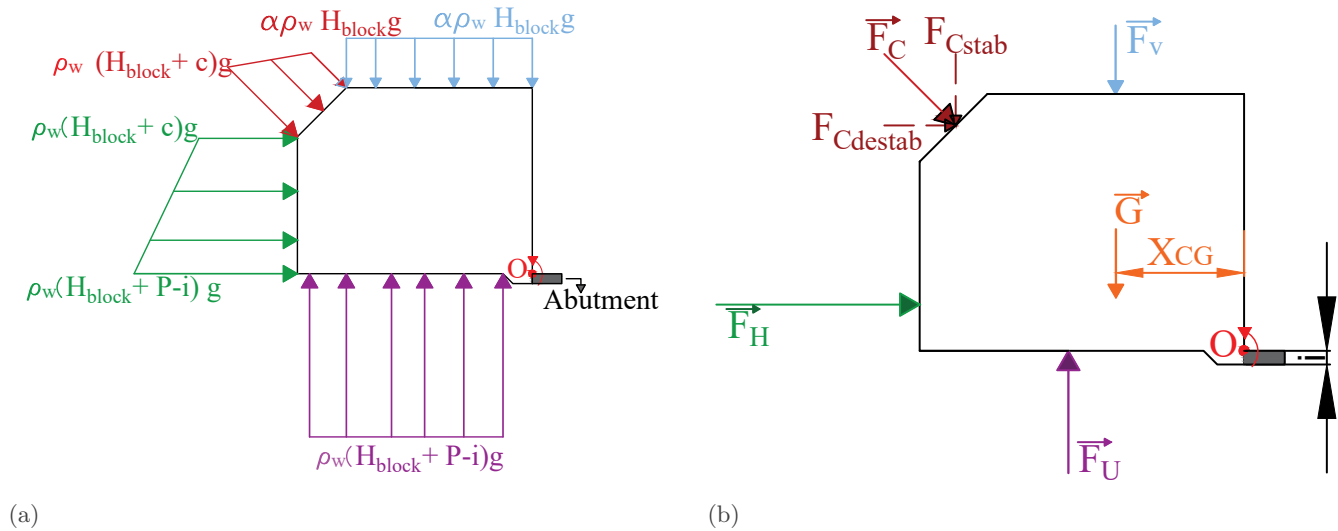


Figure 10: (a) Hydrostatic pressure distribution assumptions. (b) Force diagrams. The pressures shown in (a) are integrated over the corresponding surfaces. The resultant forces are: \vec{F}_U from underpressure on the bottom face, \vec{F}_H from horizontal pressure on the upstream face, \vec{F}_v from vertical pressure on the top face, and \vec{F}_c from chamfer pressure. $F_{c,destab}$ is the horizontal component of \vec{F}_c , and $F_{c,stab}$ is the vertical component. The weight \vec{G} , is applied at the centre of mass, situated at a horizontal distance X_{CG} from the rotation point O , which is at the top of the downstream abutment (this distance corresponds to the horizontal component of the vector linking the centre of mass to the axis of rotation).

4 Results

Figure 11 illustrates an experiment sequence: block's stability before tipping (a), start of tipping (b), block's fall downstream (c), and outflow after the block has fallen (d).

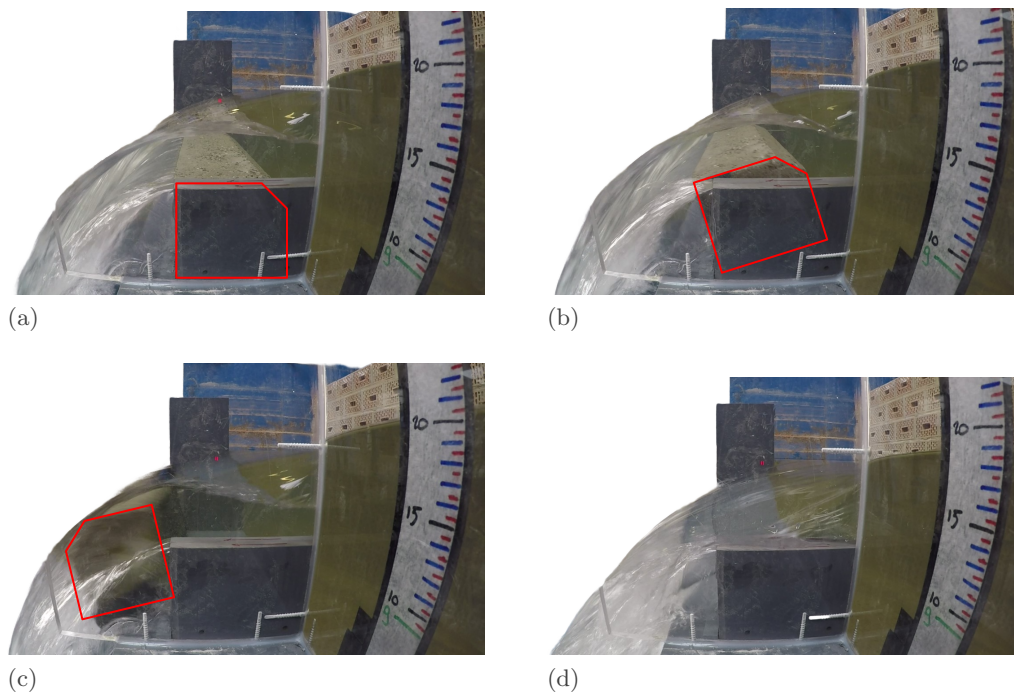


Figure 11: Picture showing the tipping of a block during experimental tests. The test corresponds to configuration 1, with block B50 placed on the side of the weir crest. The side of the block is outlined in red. (a) Block stable before destabilisation. (b) Beginning of the tipping. (c) Block falling downstream of the weir. (d) Flow after the block has fallen (5 seconds after (c)).

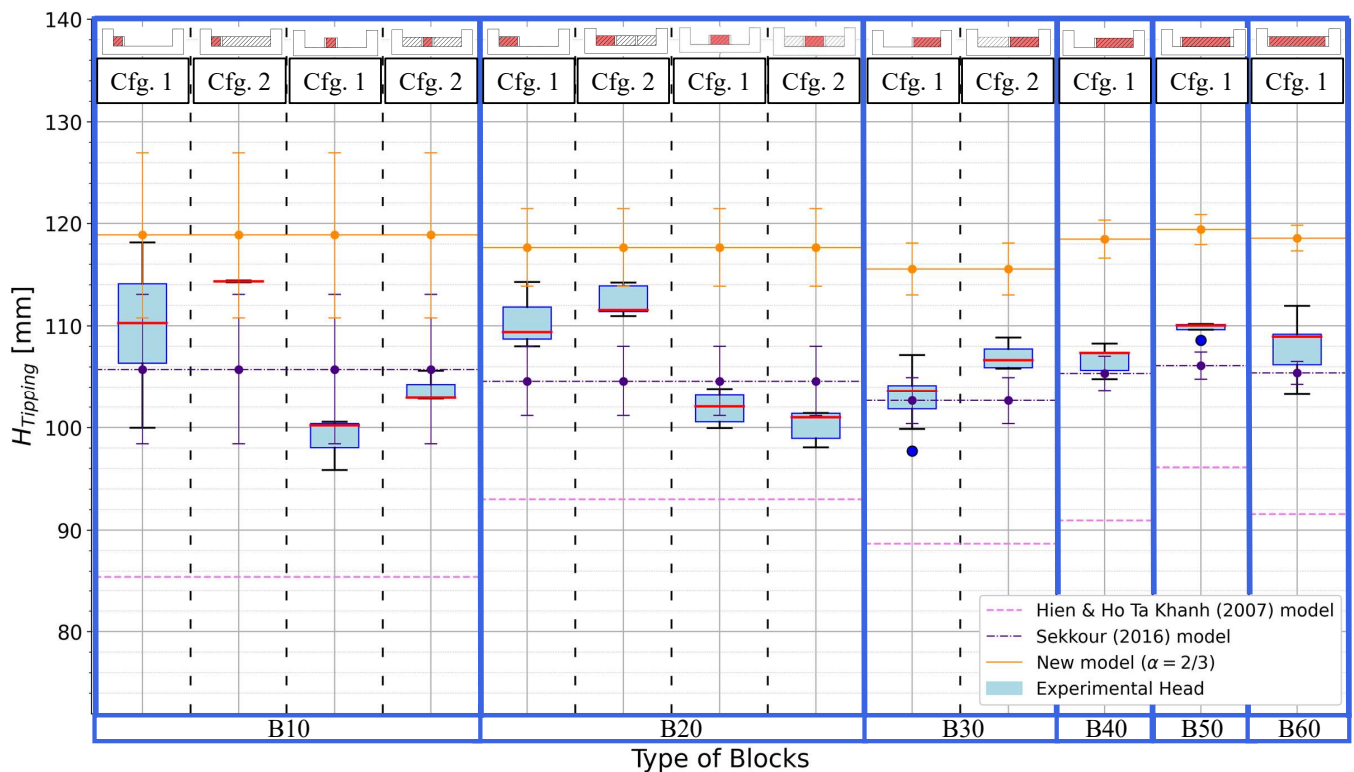


Figure 12: Experimental and theoretical tipping head $H_{Tipping}$ results for blocks B10 to B60 across different test configurations. Box plots show experimental Tipping Heads and Unstable Heads results. Theoretical results are from Hien and Ho Ta Khanh (2007) model (pink), Sekkour (2016) model (purple), and the new model (orange). Error bars represent the effect of block density uncertainty.

Figure 12 presents the experimental data for blocks B10 to B60 across various configurations, displayed as whisker boxes. These box plots illustrate the Tipping Heads and Unstable Heads (see the definition provided in Section 2) results.

The experimental results suggest that any potential influence of tested parameters on the tipping head $H_{Tipping}$ is masked by the experimental uncertainty, as illustrated by the overlapping ranges in the box plots. This is observed for different configurations (block alone on the weir vs. presence of adjacent blocks with B10, B20, B30), different positions on the weir (centre vs. side with B10 and B20), and varying block widths (from B10 to B60). Although slight differences in median values exist, the variability in repeated tests prevents any clear trend from emerging.

From theoretical predictions, it appears that the two models from the literature show differing trends in estimating the head required for block tipping. The equation proposed by Hien and Ho Ta Khanh (2007) consistently underestimates the tipping heads, with discrepancies ranging from 8.29% to 27.67% between the theoretical value and the maximum value of the whisker boxes. In contrast, the formula by Sekkour (2016) provides a closer approximation of the experimental results, but alternates between underestimations (up to 10.47%) and overestimations (up to 5.16%) of the maximum value of the data.

Conversely, the new model consistently overestimates the tipping heads, with discrepancies ranging from 0.63% to 18.20% compared to the maximum values observed in the tests. The assumptions made in the model, particularly the parameter $\alpha = 2/3$, result in safe theoretical values relative to the test data. Adjusting the model to better match the overall test results for optimal block geometry would compromise dam safety, as it would lead to underestimating the tipping heads for certain configurations, despite aligning more closely with others. Therefore, the decision was made to prioritize safety by retaining the current model, which provides a more conservative prediction. An additional advantage of this formula is its independence from the test data, meaning it is not calibrated to them.

To facilitate practical use of the analytical model, Eq. (4) was applied to a standard block geometry, based on the aspect ratios defined by Lempérière and Vigny (2013) and consistent with those used in the present experiments. These ratios are:

$$e = \frac{12}{10}P \quad ; \quad c = \frac{1}{4}P \quad ; \quad s = \frac{1}{10}P \quad ; \quad i = \frac{1}{20}P. \quad (5)$$

By substituting these expressions into Eq. (4), we obtain a specific form of the equation for this geometry:

$$H_{Tipping}^* = P \cdot (1.075 \cdot 10^{-3} \cdot \rho_b - 1.304). \quad (6)$$

This simplified equation is not based on additional assumptions but is a direct application of the general model to the defined standard geometry, allowing straightforward determination of the block height for given values of ρ_b and P .

5 Discussion

5.1 Validity of the analytical model and experimental results

Results from the analytical equations highlight that the accuracy of predictions is generally better with Sekkour (2016) equation. However, the main issue with this formula lies in its inconsistency: it alternates between overestimating and underestimating the results. This variability is problematic, as it raises concerns about the reliability of the predictions, particularly in flood control contexts where safety and vigilance are critical. In contrast, the new model, while not necessarily offering higher accuracy, ensures that predictions remain consistently on the safe side regarding dam overtopping. This is a significant advantage, as it provides confidence in the reliability of the results.

Furthermore, the new model is conceptually more robust. It accounts for the continuity of pressures on the block faces, offering a more physically realistic representation of the problem —an aspect missing in the other models. Additionally, the assumption of the coefficient $\alpha = 2/3$ has a clear physical basis, as it reflects a hydrostatic pressure field and critical water depth. This value ensures a safe representation of all experimental results without requiring calibration of the formula to specific test, making the model independent of experimental conditions. The assumption of a uniform pressure distribution on the block crest is debatable; other assumptions, such as a distribution varying linearly or an intermediate option, might better reflect reality. Experimental tests focusing on block crest pressure distribution are needed to determine a more realistic assumption.

Scale effects are expected to be limited in this study, as the experiments were conducted on a relatively large 1:10 scale model with water heads well above the threshold (~ 3 to 7.5 cm) below which such effects typically become significant (Erpicum et al., 2016; Ettema et al., 2000).

Figure 12 shows the theoretical tipping heads with the error bars representing the density uncertainty. For block B10, with a density $2302.5 \pm 74.5 \text{ kg/m}^3$, this uncertainty introduces a $\pm 7.5 \text{ mm}$ error in the tipping head, demonstrating the high model's sensitivity to density. According to Eq. (4), the error induced by density uncertainty on the tipping head is proportional to the block height. Therefore, precise density measurement is crucial during construction.

A crucial aspect of the design is managing friction between the block and the separating walls. This factor was excluded from the analytical modelling to simplify developments, assuming that adequate clearance would minimise contact.

Repeating the tests with different configurations and positions helps to understand the influence of the clearance between the block and separator walls, as well as the effect of the watertight seal on block tipping. In the initial weir configuration (0.66 m wide), three tests were conducted with block B20 centred and no clearance. No tipping occurred because the block was jammed against the side walls. In a second configuration, with block B10 centred on the weir and no clearance, the six test outcomes ranged from 124.35 mm to 136.52 mm (Figure 13a). These higher tipping head values resulted from the adjacent blocks being fixed in a way that constrained the block between the walls. After adjusting the fixation of the adjacent blocks to avoid constraining the free block, the tipping heads fell within a range of 102.81 mm to 105.62 mm (results shown in Figure 12). This adjustment represents a difference of approximately 25% compared to the scenario where the block was constrained and a variation of 12.92% relative to the theoretical head predicted by the new model. It appears, therefore, that the lack of clearance between the block and the separator walls delays the tipping of the blocks or may completely prevent it.

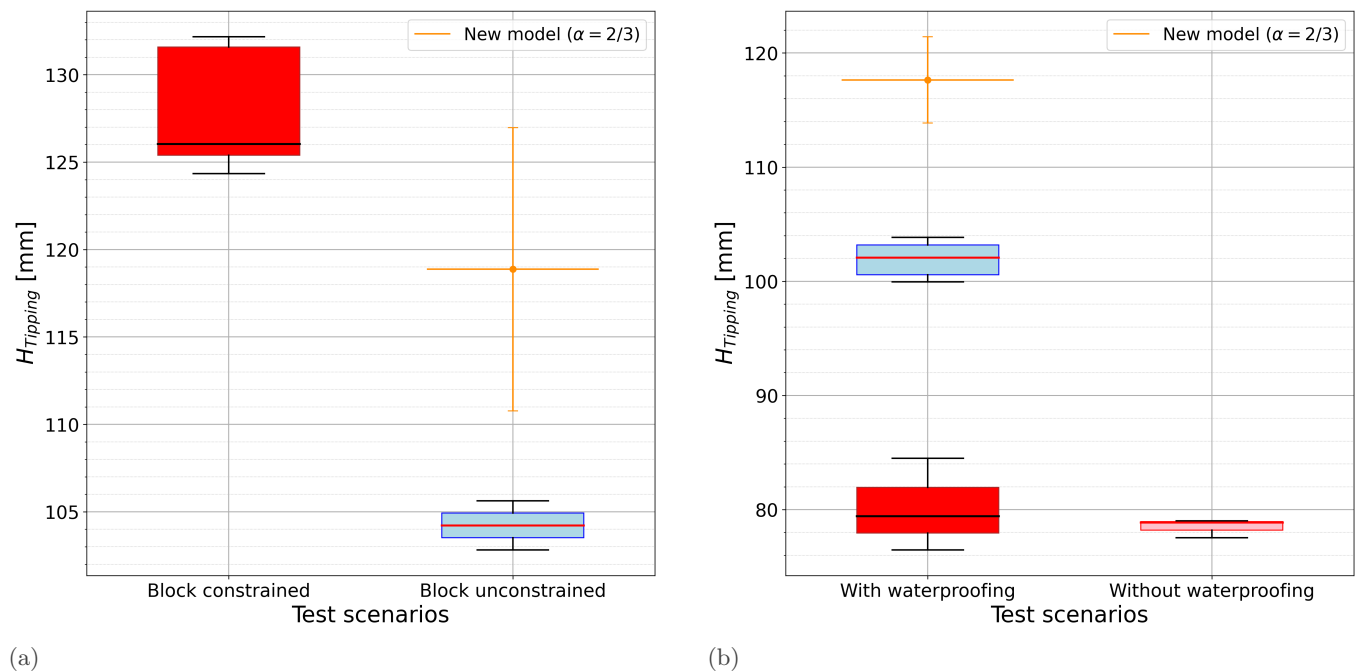


Figure 13: (a) Experimental tipping head ($H_{Tipping}$) results for block B10 centred on the weir in configuration 2. Test scenarios: (1) 6 tests with the block constrained between the walls due to fixed adjacent blocks, and (2) 3 tests with the block unconstrained after adjusting the fixation of the adjacent blocks (results shown in Figure 12). (b) Experimental tipping head ($H_{Tipping}$) results for block B20 centred on the weir in configuration 1 with a large 6 mm gap. Test scenarios: (1) 7 tests ranging from 99.94 to 103.84 mm (results shown in Figure 12), suggesting that the waterproofing remained in place, and 3 tests ranging from 76.46 to 84.50 mm, suggesting that the waterproofing was washed out; and (2) 3 tests without waterproofing.

When widening the weir (from 0.66 m to 1.224 m), special attention was given to measuring clearance between the blocks and the separator walls. Positioned centrally, the 20 cm-wide block was placed within a total available space of 20.6 cm between the separating walls, leaving a 6 mm gap (3 mm on each side). With this clearance, the block tipped three times at head values between 76.46 mm and 84.50 mm (Figure 13b), *i.e.*, a difference of about 20% compared to the results shown in Figure 12. This represents a variation of 39.21% between the maximum value (84.50 mm) and the theoretical head calculated using the new model. These lower head values correspond to the heads needed to tip a block without waterproofing (*i.e.*, without the plastic sealing strips), Figure 13b. This similarity suggests that, in the three tests where head values ranged from 76.46 mm to 84.50 mm, the waterproofing initially placed was washed out

before block tipping. Similar results were observed for block B60 when the available width was 60.5 cm, corresponding to a 6 mm gap. These examples demonstrate that excessive clearance between blocks and separator walls leads to early block tipping.

The influence of the watertight seal system and its position on tipping may also be important. To understand its effect and minimize operator dependency in the setup (thus avoiding results and interpretations being overly dependent on how the operator carried out the tests), 18 tests were conducted with three different operators (Figure 14). These tests were conducted for block B30 positioned at the side of the weir in configuration 1, with a clearance of 3 mm. An initial set of three tests was carried out, followed by each operator conducting five tests according to the same procedure described in Section 2.2. The primary difference among the three operators was in how they positioned the watertight seals. It was observed that Operator 1 placed the sealing strip further upstream compared to the other operators, before the strip could be trapped between the block and the separator wall. Operator 2 placed the sealing strip further downstream but did not align it with the downstream face of the block. Operator 3, on the other hand, ensured that the sealing strip was aligned with the downstream face of the block.

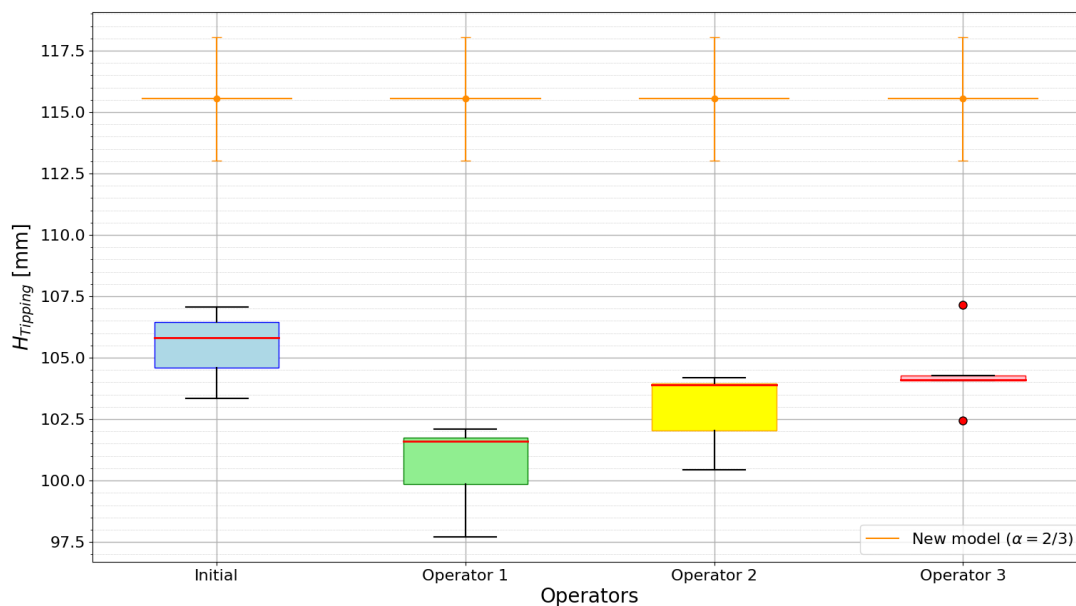


Figure 14: Experimental tipping head ($H_{Tipping}$) results for block B30 positioned at the side of the weir in configuration 1, showing results for three operators (five tests each) compared to a baseline of three tests.

From these tests, it is evident that the placement of the watertight seal influences the tipping of the block. The further downstream the seal is positioned—meaning it is more tightly wedged between the block and the adjacent wall—the higher the head required for the block to tip. Despite this, the variability between operators remains within approximately 9%. This level of variability is comparable to the experimental uncertainty observed when repeating tests with the same operator in different block configurations, and therefore does not increase the overall uncertainty of the results. All these results are included in the box plot in Figure 12.

Figure 14 includes the tipping head predicted by the new model. As already shown, the model consistently overestimates the results obtained by all three operators. The prediction is closest to the results of Operator 3, who aligned the seal with the downstream face of the block, suggesting that the model performs best when the seal is correctly placed. However, it still provides a conservative estimate in all cases. From a design perspective, this means that small misalignments in the sealing strip do not require the application of additional safety margins, as the model already provides conservative predictions that support dam safety.

These tests highlight the need for a clearance (ranging from 2 to 4 mm in the tests performed), but not too wide (from 6 mm), between the blocks and the walls. This is a crucial consideration to ensure proper functioning. To prevent leaks, a thick plastic or rubber sealing strip should be installed in the gap between the blocks and the walls to ensure watertightness. The position of the watertight seal should allow the block to tilt freely, but it appears that there is no need for precise placement, as there is no significant difference in the tipping head results.

This study analysed blocks of different widths but with constant lengths. Thus, the design methodology did not account for fuse blocks of varying lengths on the same weir. Literature (ICOLD, 2010) suggests that using elements of different lengths can create multiple tipping levels, though this is not essential. The proposed model does consider

block length, technically allowing for a generalisation in such cases. However, no experiments have verified whether this model safely predicts results for blocks of varying lengths. Therefore, further experimentation is needed to validate the proposed relationship.

The blocks in operation on Gaskaye and Wedbila dams have the same geometry as those designed by Lempérière and Vigny (2013) (Figure 15). Therefore, the results obtained from the new analytical model can be compared with the tipping head values reported in previous studies (Kabore et al., 2015; Hydrocoop, 2013). For the Gaskaye dam, the density of the concrete blocks varies between 2310 kg/m³ and 2340 kg/m³. The tipping heads calculated with the new analytical model are provided in Table 4. The tipping heads predicted by the new analytical model are higher than those expected by Kabore et al. (2015), with a maximum variation of 18.86%.

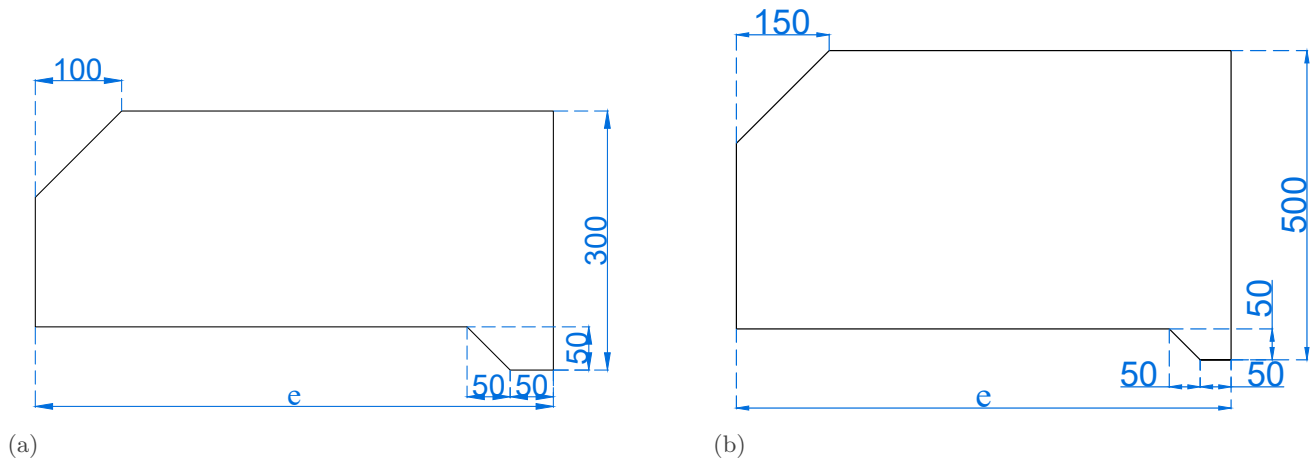


Figure 15: Cross-section of the block geometry (dimensions in mm): (a) Blocks of Gaskaye dam (based on Kabore et al. (2015)). (b) Blocks of Wedbila dam (based on ODE et al. (2009)). The block length e is given in Table 1.

Table 4: Tipping head $H_{Tipping}$ values for the Gaskaye dam regarding the block length e . Comparison between the values from Kabore et al. (2015) and those predicted by the new analytical model.

Gaskaye dam					
Lenght e [cm]	55	60	67.5	75	90
$H_{Tipping}$ [cm] from Kabore et al. (2015)	50	54.6	60.3	64.8	71.2
$H_{Tipping}$ [cm] from the new analytical model ($\rho_b = 2310$ kg/m ³)	58.03	61.52	65.69	68.87	73.22
$H_{Tipping}$ [cm] from the new analytical model ($\rho_b = 2340$ kg/m ³)	59.43	62.99	67.25	70.49	74.92

Regarding the blocks of the Wedbila dam, no information is available on the block density. To estimate the tipping heads using the new model (Table 5), a density of 2300 kg/m³ is assumed. The tipping heads predicted by the new model are higher than those expected by Hydrocoop (2013) with a maximum variation of 23.28% when assuming a density of 2300 kg/m³. However, to achieve similar order of magnitude for the tipping head, the density would need to be around 2100 kg/m³, which seems low for a concrete block.

Table 5: Tipping head $H_{Tipping}$ values for the Wedbila dam regarding the block length e . Comparison between the values from Hydrocoop (2013) and those predicted by the new analytical model ($\rho_b = 2300$ kg/m³).

Wedbila dam							
Lenght e [cm]	78	82	85	89	94	98	103
$H_{Tipping}$ [cm] from Hydrocoop (2013)	66	70	74	78	82	86	90
$H_{Tipping}$ [cm] from the new analytical model	81.36	85.75	88.83	92.67	97.07	100.30	104.00

For these two dams, the design of the blocks was carried out through a collaboration between HydroCoop France and IFEC Consulting Engineers (Hydrocoop, 2013; Kabore et al., 2015). However, no information is provided regarding

whether the blocks were dimensioned analytically or experimentally. If these results were obtained experimentally, it is logical to observe that the new analytical model produces higher estimates, as it overestimates the tests conducted in this study to ensure a safe design. The variation between the experimental results from this study and the analytical model ranges from 0.63% to 18.20%, with an average variation of 8.31%. Consequently, it can be noted that the discrepancies between the dam designs and the analytical formula (18.86% and 23.28%) remain higher than those observed in this study. This suggests that the formula developed in this work consistently ensures a safe design regarding dam overtopping.

5.2 Practical implications and limitations of fuse blocks

While fuse blocks offer several advantages for increasing spillway capacity and ensuring dam safety, some limitations should be acknowledged and discussed.

One concern relates to the intensity of discharges generated when the blocks tip and the potential consequences downstream. Before tipping, water already flows over the block, and discharge increases progressively with the upstream head. Tipping does not cause a sudden transition from no flow to a high discharge. Instead, it results in a discharge increment, Q_{Tipping} , as the head now acts directly on the spillway crest, producing a new discharge rate, Q_{overflow} . To avoid sudden large discharges due to the simultaneous tipping of all blocks, a staged tipping sequence can be implemented. This can be achieved by varying the cross-sectional geometry of the blocks, so that each tips at a different water level. This allows for a gradual increase to maximum discharge.

The model is conservatively designed to overestimate the tipping head, thereby ensuring dam safety with respect to overtopping. However, if blocks tip earlier than predicted, this may lead to more frequent overflows, which represents a limitation of the system. Still, dam safety remains the priority, as the flows generated by tipping blocks are less hazardous than those resulting from dam failure. To further reduce flood risks, designing blocks to tip at different water levels can help mitigate the impacts by spreading the release over time and reducing the intensity of the resulting flow.

Even if blocks tip earlier than predicted, they remain useful. Tipping only occurs after submersion, so the usable storage—equivalent to the block height—is always preserved provided that only limited floods occur. According to the new model (Eq. 6), the predicted tipping head is approximately equal to the block height, P . Experimental tests showed an overestimation of tipping head ranging from 0.63% to 18.20%. Therefore, even if tipping occurs slightly earlier than predicted, *i.e.* for floods smaller than the design flood but still important in terms of overflow depth and discharge, the blocks still provide a reliable increase in storage capacity.

When the blocks tip, the head acting on the spillway nearly doubles ($\approx 2P$), resulting in a substantial increase in discharge capacity. This aligns with ICOLD's (2010) conclusion that concrete fuse blocks can double the extreme flood discharge using approximately the same amount of concrete as a fixed raised crest.

The effect of floating debris on the tipping head was beyond the scope of this study. Nonetheless, model tests reported by ICOLD (2010) indicate that floating debris does not significantly affect water levels at the moment of tilting, suggesting a limited influence on the block's tipping behaviour.

ICOLD (2010) noted that replacing toppled blocks may take time, temporarily reducing storage capacity. To address this, they proposed using temporary flashboards—such as wooden planks supported by steel tubes—that can be quickly installed. This can be done as early as the day after the flood, provided that fixing holes have been pre-drilled and low-cost materials are available (ICOLD, 2010).

This study did not investigate the potential structural consequences of block tipping, either on the weir itself or downstream. Yet this is a critical aspect for real-world applications. The experiments were conducted on a broad-crested weir with a vertical downstream face, and it remains unclear how block tipping would behave with a sloped downstream face. Depending on the flow velocity and the characteristics of the overflowing nappe, the block could potentially slide along the slope, fall with a greater impact, or even be carried away downstream without touching the slope. Since tipping occurs only after submersion, a water layer cushions the fall. However, the block's weight still induces an impact force on the downstream surface. Observations during testing showed that blocks were slightly displaced by the flow after tipping, but only over short distances. Given the flow velocities and resulting pressures, some downstream movement may be expected on prototypes. The potential for damage to the structure or erosion downstream warrants further investigation. To our knowledge, no full-scale fuse block has yet tipped in practice, so no real-world data are available.

6 Simple design method

From Eq. 6, a simple design methodology in three steps is proposed to determine the block height depending on block density and dam safety values.

First, the maximum reservoir head compare to spillway crest H_{HRWL} is chosen, which is the distance from the spillway crest to the highest reservoir water level (HRWL) or the dam safety level. While fuse blocks increase water storage capacity, the primary role of the spillway is to ensure safety during floods by preventing overtopping, so the design must account for this limit level.

Second, a safety margin H_{safe} may be considered to account for uncertainties. The sum of the predicted tipping head and block height, $P + H_{Tipping}$, should not exceed the distance $H_{HRWL} - H_{safe}$ (Figure 16).

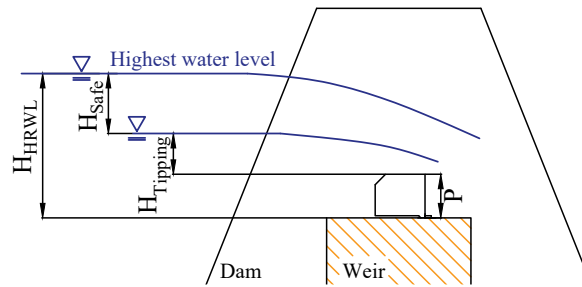


Figure 16: Diagram illustrating the key dimensions for the design of fuse blocks: the maximum head in the reservoir H_{HRWL} , the safety margin H_{safe} , the block tipping head $H_{Tipping}$, and the block height P .

Finally, from the maximum upstream head $P + H_{Tipping} = H_{HRWL} - H_{safe}$, Eq. (6) can be used to select a pair (ρ_b, P) for designing the blocks. The design table in Table 6 helps to easily find the block height for a given density, H_{HRWL} and H_{safe} . The table's horizontal axis represents block density, and the vertical axis represents the safety margin expressed as a percentage of H_{HRWL} . The table output is the block height also expressed as a percentage of H_{HRWL} . For instance, if the table indicates 45% and H_{HRWL} is 1 m, the block height is 45 cm. The other dimensions of the block are easily determined using the relationships given in Eq. (5).

Table 6: Design table for fuse blocks: the density (ρ_b [kg/m³]) is represented on the horizontal axis, and the safety margin (H_{safe}/H_{HRWL} [%]) on the vertical one. The output shows the block height (P/H_{HRWL} [%]). Both the safety margin and the block height are expressed as a percentage of H_{HRWL} .

		Density ρ_b [kg/m ³]												
		2200	2225	2250	2275	2300	2325	2350	2375	2400	2425	2450	2475	2500
H_{safe}/H_{HRWL} [%]	0	45	45	45	45	45	45	45	45	45	40	40	40	40
	5	45	45	45	45	40	40	40	40	40	40	40	40	40
	10	40	40	40	40	40	40	40	40	40	40	35	35	35
	15	40	40	40	40	40	35	35	35	35	35	35	35	35
	16	40	40	40	40	35	35	35	35	35	35	35	35	35
	17	40	40	40	35	35	35	35	35	35	35	35	35	35
	18	40	40	35	35	35	35	35	35	35	35	35	35	35
	19	40	35	35	35	35	35	35	35	35	35	35	35	30
	20	35	35	35	35	35	35	35	35	35	35	35	30	30
	21	35	35	35	35	35	35	35	35	35	35	30	30	30
	22	35	35	35	35	35	35	35	35	35	30	30	30	30
	23	35	35	35	35	35	35	35	35	30	30	30	30	30
	24	35	35	35	35	35	35	35	30	30	30	30	30	30
	25	35	35	35	35	35	35	30	30	30	30	30	30	30

It should be noted that, according to the design table, a 25 kg/m³ variation in block density necessitates a 5%

reduction in height to ensure safety. Thus, it is crucial to ensure accurate densities, particularly for tall blocks. Special attention should be paid to the concrete mix, and/or sample blocks must be produced to measure and verify their density during construction.

7 Conclusions

In this study, we analysed the conditions for fuse block tilting in reservoir conditions. Six blocks designed according to Lempérière and Vigny (2013) recommendations with varying widths were studied experimentally in two test configurations: placed alone on the sill or with adjacent blocks fixed beside them and two different positions: at the centre or on the side of the weir.

A new analytical model, based on momentum equilibrium, was developed to predict block tilting head. It includes a parameter α , representing the percentage of the upstream head acting on the block crest surface. Compared to the existing models from literature, the new model considers the exact block geometry and is based on continuous pressure distribution at block faces transition. Considering hydrostatic pressure and critical water depth on the block upstream face (α equal to $2/3$) was found to provide safe results. The assumptions made in the development of this new model allow for a physical representation of the problem, independent of the experimental results. While it does not aim to be more precise than the models in the literature, it ensures systematically safe predictions compared to experimental tests.

The tests showed that the absence of any friction between the block and the separating wall is crucial to ensure proper operation. However, excessive clearance between the blocks and the separating walls can lead to premature tipping. This issue requires particular attention when installing the blocks on the weir. A simple and effective system for waterproofing the vertical gap between the fuse block and separating walls is the placement of a thick plastic or rubber sealing strip. In addition, maintaining an adequate clearance (between 2 to 4 mm, as observed in our tests) is essential for proper functioning, as it ensures the block tilts freely without excessive movement that could lead to premature tipping.

A practical design table for fuse blocks was developed. This table allows practitioners to determine the height of fuse blocks based on density and required flood level safety margin. Simple relationships enable calculating other block dimensions from this height.

To reduce the risk of intense discharges following block tipping, a staged tipping sequence using blocks with varying cross-sections could be implemented. While the study focused on overtopping safety to prevent dam failure and its consequences on local populations, such a strategy would also help mitigate flood risks in case of earlier-than-expected tipping.

This study rationalises the design of safe and efficient fuse blocks for small dams. These blocks offer a low-cost solution to increase storage—by an amount equivalent to their height—while ensuring protection against overtopping. Yet, even though these results constitute a solid first step, further experimentation could complement this research. Conducting experiments to test the model's accuracy with blocks of varying lengths e would be valuable for validating its predictive capabilities. Additional research is needed to better understand potential structural or erosion-related impacts downstream.

Acknowledgements

The authors would like to express their gratitude to Grégory Thonard and Maxime Mathieu for their invaluable assistance in setting up and conducting the experiments. We would also like to thank Clément Delhez and Alexandre De Becker for their contribution to the experimental work.

Funding

The support of the Joseph Deprez Foundation is gratefully acknowledged.

Author contributions (CrediT)

KA: Conceptualisation, Data curation, Formal analysis, Investigation, Methodology, Validation, Writing – original draft, Writing – review and editing. SM: Formal analysis, Writing – original draft, Writing – review and editing. PA: Writing – review and editing. BD: Writing – review and editing. MP: Writing – review and editing. SE: Conceptualisation, Validation, Funding acquisition, Supervision, Writing – original draft, Writing – review and editing

Use of AI

During the preparation of this work, the author(s) used DeepL Write and ChatGPT in order to check grammar and spelling. After using this tool/service, the author(s) reviewed, edited, made the content their own and validated the outcome as needed, and take(s) full responsibility for the content of the publication.

Data access statement

The data acquired in the study will be made available on reasonable request.

Conflict of interest (COI)

There is no conflict of interest.

Notations

Name	Symbol	Unit
Upstream width (in flow direction)	b	m
Downstream width (perpendicular to flow direction)	B	m
Block chamfer height and length	c	m
Discharge coefficient	C_d	-
Norm of the gravitational acceleration	g	m/s ²
Upstream head of the block	H_{block}	m
Maximum reservoir head compared to spillway crest	H_{HRL}	m
Upstream tipping head of the block	$H_{Tipping}$	m
Upstream tipping head for the defined standard block geometry	$H_{Tipping}^*$	m
Safety margin	H_{safe}	m
Height of the block underpressure chamber	i	m
Mass of the block	M	kg
Block height	P	m
Width of block supports delimiting the underpressure chamber	s	m
Reduction factor of vertical pressure applied on the block (new model)	α	-
Reduction factor of vertical pressure applied on the block (Hien and Ho Ta Khanh (2007) model)	β	-
Specific weight of the block	γ_b	kN/m ³
Specific weight of water	γ_w	kN/m ³
Water density	ρ_w	kg/m ³

References

- Durand, J., Royet, P. and Mériaux, P. (1999). *Technique des petits barrages en Afrique sahélienne et équatoriale*, Irstea, EIER.
- Ercicum, S., Tullis, B.P., Lodomez, M., Archambeau, P., Dewals, B.J. and Pirotton, M. (2016). Scale effects in physical piano key weirs models. *Journal of Hydraulic Research*, **54**(6), 692–698. DOI:10.1080/00221686.2016.1211562.
- Ettema, R., Arndt, R., Roberts, P. and Wahl, I. (2000). *Hydraulic Modeling: Concepts and Practice*, American Society of Civil Engineers.
- Güven, A. and Aydemir, A. (2020). *Dams*, 1–25, Springer International Publishing, Cham.
- Hien, T.C. and Ho Ta Khanh, M. (2007). Report on fuseplugs with uplift model tests, Technical report, Ho Chi Minh city University of Technology, Faculty of Civil engineering, Department of Water resources engineering.

- Hydrocoop (2013). Low cost technologies to improve reservoirs storage - dam engineering, Blog post on *Dams, Piano Keys Weirs, Tidal Energy & Energy Storage* <https://www.hydrocoop.org/reservoirs-storage-low-cost-technologies/>, accessed on 11.05.2024.
- Hydrocoop (2015). Deversoirs économiques pour augmenter sécurité et stockage : les blocs fusibles, Blog post on *Crues et déversoirs* <https://fr.hydrocoop.org/deversoirs-economiques-pour-augmenter-securite-et-stockage-les-blocs-fusibles/>, accessed on 11.04.2025.
- Hydrocoop (n.d.). Hydrocoop - non profit organization – expertise in dams, tidal energy and energy storage, <http://www.hydrocoop.org/>, accessed on 01.08.2024.
- ICOLD (2010). Appendix 3 - concrete fuse plugs. *Cost savings on dams - Economies dans les barrages*, **144**, 191–196.
- ICOLD (2011). Constitution / statuts, https://www.icold-cigb.org/FR/cigb/dossiers_institutionnels.asp, accessed on 04.09.2025.
- ICOLD (2016). Bulletin 157: Small dams: Design, surveillance and rehabilitation, Technical report, ICOLD, Paris.
- ICOLD (2023). General synthesis - world register of dams, https://www.icold-cigb.org/article/GB/world_register/general_synthesis/general-synthesis, accessed on 11.05.2024.
- Kabore, M., Millogo, F., Nacanabo, A. and Vigny, J.P. (2015). Implementation of concrete fuse plugs on gaskaye dam to increase the reservoir capacity, In: *Proceedings of ICOLD 2015 — Stavanger, Norway*.
- Lempérière, F. (2017). Dams and floods. *Engineering*, **3**, 144–149. DOI:10.1016/J.ENG.2017.01.018.
- Lempérière, F. and Vigny, J. (2013). Économie et sécurité des déversoirs du burkina faso, Publication by HydroCoop France, presented at the 1er Congrès National des Barrages, Burkina Faso. Accessed on 11.29.2023.
- National Performance of Dams Program (2018). Dam failures in the u.s., Technical Report NPDP-01 V1, Department of Civil & Environmental Engineering, Stanford University, Stanford, California.
- ODE, Association Eau Sans Frontières, HydroCoop France and IFEC (2009). Plan de recollement des travaux de rehaussement du déversoir du barrage de wedbila, - Vue en plan du seuil, coupe transversale d'un bloc et du déversoir.
- Pinto, W.L.H. and Ferreira Fais, L.M.C. (2023). The small dams safety index (sdsi): a tool for small dams safety assessment. *International Journal of River Basin Management*, **21**(3), 551–558. DOI:10.1080/15715124.2022.2047711.
- Salunkhe, S.S., Kolhe, P.R., Bhange, H.N., Jadhav, V.D. and Ayare, B.L. (2020). Application of c language to design chute spillway. *International Journal of Current Microbiology and Applied Sciences*, **9**(10), 399–408. DOI: 10.20546/ijcmas.2020.910.049.
- Sekkour, I. (2016). *Contribution à l'étude des déversoirs auto-stables*, Master's thesis, Université Mohamed Khider, Biskra, Algeria.
- World Bank (2021). Small dam safety. good practice note on dam safety; technical note 4, Technical report, World Bank, Washington, DC, license: CC BY 3.0 IGO.